Literature Thesis
Some mathematical models for wound healing in soft tissues

Olmer van Rijn

January 19, 2010

Contents

Chapter 1

Introduction

For every animal's survival it is vital for its body to be able to repair injured parts. When injured the body responds with a series of events, beginning with containing the damage and working towards recovery. The biological model described in [1] and summarized below describes the various stages of the wound healing process.

In medicine the cutaneous wound healing process is generally divided into three overlapping stages. These stages mainly consist of (1) inflammation, (2) granulation tissue formation and (3) wound closure. In the inflammation stage the body attempts to contain the damage. The inflammatory process tries to either destroy, dilute or wall off the injurious agent. Along with removing the cause of the injury it starts off the healing process, [1].

In stage two granulation tissue is formed in the wound. Fibroblast invade the wound area and contract the surrounding tissue (extra cellular matrix) to ensure that new small blood vessels, capillaries, can be formed (angiogenesis). As new blood capillaries are formed, oxygen and nutrients can once again be transported to the wound side.

Finally when the tissue is provided with enough oxygen and nutrients the process of wound closure starts. Cells in the epidermis, which consist of mainly keratinocytes, start regenerating the upperlayer of the wound. Usually the skin can not be replaced fully and some marks are left where the wound was located, like scars.

The processes of granulation tissue forming and wound closure do not take place at the same place in the wound. The former is located in the dermis, the latter is limited to the epidermis. The epidermis and the dermis consist of different type of cells and are seperated by a so-called basal membrane, see also Figure 1.1.

In this literature thesis we present a selection of the currently available mathematical models that seek to describe the biological processes of wound healing as well as possible. The healing process is very complex and many factors contribute to it, therefore simplifications have to be made. In Chapter 2 we give a detailed description to which mathematical wound healing models this has led.

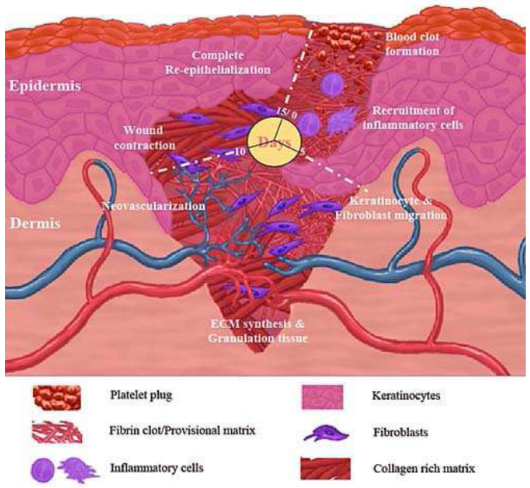

Figure 1.1: A schematic of the events during wound healing. The dermis and epidermis are illustrated. The picture was taken with permission from http://www.bioscience.org/2006/v11/af/1843/figures.htm

Such models could give more insights on how the process of wound healing works. These insights might lead to treatments that reduce healing time, e.g. the use of certain hormones to speed up the healing process. Also scars and other deformations due to incomplete healing might be prevented.

For some of the models, one for each stage of the wound healing process, we have done simulations. The results are shown and discussed in Chapter 3. Finally, in Chapter 4, possible improvements of the models are put forward as we discuss future work that can be done in this topic.

Chapter 2

Mathematical Models

The mathematical model for wound healing is usually seperated in three distinct parts respresenting the three stages of wound healing. There are several approaches on how to model each different stage, some of which will be discussed in the following chapter. The three stages that are modelled are wound contraction, angiogenesis and wound closure. The inflammation stage mentioned in Chapter 1 is not taken into account, since it contains the damage and only after inflammation the real healing process starts.

First two wound contraction models, see section 2.1, will be presented. The second model extends the first by adding an extra aspect of wound contraction. Next, see section 2.2, two models on angiogenesis will be discussed. They differ greatly in the way they try to model the growth of new blood vessels in the wound. For the third fase, wound closure, also two models are presented in section 2.3. In section 2.4 a study that attempts to combine models of the three stages is briefly discussed.

2.1 Wound contraction

In the wound contraction phase fibroblast invade the wound and contract the extracellular matrix (ECM). This process is vital to assure that new blood vessels can be formed in the wound during angiogenesis. Also it decreases the area of contact between the wound and its surroundings, thus reducing the chance of contamination. This process is located in the dermis.

2.1.1 Murray and Tranquillo

Aside from the (slightly adapted) linear viscoelastic equations, which model the displacement of the ECM, the model due to Tranquillo covers the change of both the fibroblast concentration and the ECM density over time. The ECM density is assumed to be affected only by ECM production and by passive movement due to its own displacement, [2]. The first process is assumed to be proportional

to the fibroblast concentration and the difference between the equilibrium ECM density and the ECM density itself, [8]. The resulting equation for the ECM density then becomes

$$\frac{\partial \rho}{\partial t} + \nabla \cdot (\mathbf{u}_t \rho) = bn(\rho_0 - \rho), \tag{2.1}$$

where ρ represents the ECM density, n the fibroblast concentration, $\mathbf{u}$ the displacement vector, ρ_0 the equilibrium ECM density, b the ECM production rate and where the term $\nabla \cdot (\mathbf{u}_t \rho)$ accounts for the passive movement.

The equation for the fibroblast concentration is similar to (2.1). It differs in the fact that fibroblast are also assumed to move actively due to diffusion, [2]. This gives us the equation for the fibroblast concentration as

$$\frac{\partial n}{\partial t} + \nabla \cdot (\mathbf{u}_t n - D_n \nabla n) = rn(n_0 - n), \tag{2.2}$$

where D_n denotes the diffusion coefficient, r the fibroblast production rate and n_0 the equilibrium fibroblast concentration.

As said, to model the displacement of the ECM the linear viscoelastic equations are used. These equations are slightly adapted to also incorporate cell traction. Cell traction is assumed to be proportional to both the ECM density and the fibroblast concentration, [8]. The force equilibrium is thus given by

$$\nabla \cdot \left[\mu_1 \epsilon_t + \mu_2 \theta_t \mathbf{I} + \frac{E}{1+\nu} \left(\epsilon + \frac{\nu}{1-2\nu} \theta \mathbf{I} \right) + \frac{\tau \rho n}{1 + \lambda n^2} \right] = s \rho \mathbf{u}, \tag{2.3}$$

where μ_1, μ_2, E and ν denote respectively dynamic and kinematic viscosity, Young's modulus and Poisson's ratio. Furthermore $\epsilon = \frac{1}{2}(\nabla \mathbf{u} + \nabla \mathbf{u}^T)$ denotes the strain tensor and $\theta = \nabla \cdot \mathbf{u}$ the dilation. Also s is known as the tethering elasticity coefficient and λ is a parameters which quantifies how the cell traction depends on n, [2].

At time $t = 0$ all variables are assumed to be zero inside the wound, i.e.

$$\begin{aligned} n(\mathbf{x}, 0) &= 0 \\ \rho(\mathbf{x}, 0) &= 0 \\ \mathbf{u}(\mathbf{x}, 0) &= \mathbf{0} \end{aligned}$$

for $x \in \Omega_w$. This corresponds to all fibroblasts and extra cellurar matrix being removed instantaneously from the wound side. Outside the wound area, $x \in \Omega_u = \Omega \setminus \Omega_w$, the displacement $\mathbf{u}$ is assumed to also be zero. Both the ECM density and fibroblast concentration outside the wound are initially assumed to be at its equilibrium, i.e.

$$\begin{aligned} n(\mathbf{x}, 0) &= n_0 \\ \rho(\mathbf{x}, 0) &= \rho_0 \end{aligned}$$

for $x \in \Omega_u$.

At the boundaries it is assumed that the displacement $\mathbf{u}$ is zero and that there is no transport of fibroblasts possible, i.e the flux is zero. The ECM density satisfies a first order hyperbolic equation and thus no boundary conditions can be prescribed, [8]. This is due to the fact that we impose a homogeneous dirichlet boundary condition on $\mathbf{u}$. Then $\mathbf{u}_t$ is always zero on the boundary and thus so is the second term on the left hand side of (2.2). Note that if we would not impose that $\mathbf{u}$ is zero on some part of the boundary, we would have to prescribe a boundary condition for ρ on that part. In that case a no-flow boundary condition should be imposed.

2.1.2 Olsen et al

The model for wound contraction proposed by Olsen et al. in [3] differs from Tranquillo's model in two ways. First it deals with the presence of myofibroblasts. These non motile cells differentiate from fibroblasts and transmit and amplify the traction forces generated by the fibroblasts, [8]. Second, the model incorporates the effects of a growth factor that triggers wound contraction.

In addition to a new equation for both the myofibroblast and growth factor concentration some differences are found in the other equations. The equation concerning the fibroblast concentration n becomes

$$\frac{\partial n}{\partial t} + \nabla \cdot \left(\mathbf{u}_t n - D_n \nabla n + \frac{a_n}{(b_n + c)^2} n \nabla c \right) = \left(r_n + \frac{r_{n,\max} c}{C_{1/2} + c} \right) \left(1 - \frac{n}{K} \right) n - \frac{k_{1,\max} c}{C_k + c} n + k_2 m - d_n n, \tag{2.4}$$

where c and m respectively denote the growth factor and myofibroblast concentration.

In addition to the model due to Tranquillo there is an extra term (see the fourth) on the left hand side which accounts for cell movement due to chemotaxis. The terms on the right hand side account respectively for proliferation (growth factor stimulated), differentiation to and from myofibroblasts and cell death.

The equation for the myofibroblast concentration is similar to the one for fibroblast concentration. But since myofibroblast are non motile, they will only move passively due to displacements in the ECM. The myofibroblast concentration thus solves

$$\frac{\partial m}{\partial t} + \nabla \cdot (\mathbf{u}_t m) = \varepsilon_r \left(r_n + \frac{r_{n,\max} c}{C_{1/2} + c} \right) \left(1 - \frac{m}{K} \right) m + \frac{k_{1,\max} c}{C_k + c} n - k_2 m - d_m m, \tag{2.5}$$

where $r_n,\ \varepsilon_r,\ K,\ k_1,\ k_2,\ d_m$ and C_k are known constants.

The ECM density ρ is effected by both fibroblasts and myofibroblasts, furthermore it is chemically enhanced by the growth factor concentration, [8]. The

equation for the ECM density is thus modelled by

$$\frac{\partial \rho}{\partial t} + \nabla \cdot (\mathbf{u}_t \rho) = \left(r_\rho + \frac{r_{\rho,\max} c}{C_\rho + c} \right) \frac{n + \eta_b m}{R_\rho^2 + \rho^2} - d_\rho (n + \eta_d m) \rho, \tag{2.6}$$

where the first term on the right hand side accounts for growth factor enhanced ECM production and the second term for ECM decay.

The growth factor is produced by both fibroblasts and myofibroblasts, furthermore it moves both actively as well as passively through the ECM. The resulting equation for the growth factor concentration then is

$$\frac{\partial c}{\partial t} + \nabla \cdot (\mathbf{u}_t c - D_c \nabla c) = \frac{k_c (n + \zeta m) c}{\Gamma + c} - d_c c, \tag{2.7}$$

where the last term on the right hand side respresents growth factor decay.

As in the model due to Tranquillo the displacement in the ECM is still modelled via adapted linear viscoelastic equations. The effect of the myofibroblasts can be found in that the last term on the right hand side in (2.3) is changed. The cell traction stresses are generated by fibroblasts, amplified by myofibroblasts and inhibited at high ECM densities, [8]. This results in an adapted term for the cell traction as

$$\frac{\tau_0 (1 + \xi m) n \rho}{R_\tau^2 + \rho^2} \mathbf{I}. \tag{2.8}$$

The force equilibrium is thus given by

$$\nabla \cdot \left[\mu_1 \epsilon_t + \mu_2 \theta_t \mathbf{I} + \frac{E}{1 + \nu} \left(\epsilon + \frac{\nu}{1 - 2\nu} \theta \mathbf{I} \right) + \frac{\tau_0 (1 + \xi m) n \rho}{R_\tau^2 + \rho^2} \mathbf{I} \right] = s \rho \mathbf{u}, \tag{2.9}$$

The initial and boundary conditions are similar to those of the model due to Murray and Tranquillo. The myofibroblasts are absent everywhere at the time of injury and only appear due to differentation from fibroblasts, [8]. The growth factor concentration is at its equilibrium inside the wound, it has been accumulated there during inflammation. Both the myofibroblast and the growth factor concentration are assumed to satisfy no-flow boundary conditions.

2.2 Angiogenesis

Angiogenesis is the wound healing phase that succeeds and partly overlaps wound contraction. During this phase new capillaries are formed in the wound area to supply the wound with the oxygen and nutrients needed to heal. This process, which takes place in the dermis, is modelled in two very different ways.

2.2.1 Maggelakis

The model due to Maggelakis, proposed in [4], assumes a positive relation between the lack of oxygen in the wound and the growth of new capillaries. The shortage of oxygen activates macrophages in the wound area, which in their turn

start the production of a growth factor that stimulates capillary regeneration, [8]. In return, the growth of new capillaries reduces the shortage of oxygen due to transport.

If we let u_1, u_2 and u_3 denote respectively the oxygen concentration, the MDGF (macrophage derived growth factor) concentration and the capillary density, the model due to Maggelakis follows as

$$\frac{\partial u_1}{\partial t} = D_1 \Delta u_1 - \lambda_{11} u_1 + \lambda_{13} u_3 \tag{2.10}$$

$$\frac{\partial u_2}{\partial t} = D_2 \Delta u_2 - \lambda_{22} u_2 + \lambda_{21} Q(u_1) \tag{2.11}$$

$$\frac{\partial u_3}{\partial t} = D_3 \Delta u_3 + \lambda_{33} u_2 u_3 \left(1 - \frac{u_3}{u_3^{\text{eq}}}\right). \tag{2.12}$$

Here the D_i are the diffusion coefficients, whereas the terms $\lambda_{11} u_1$ and $\lambda_{22} u_2$ respectively represent the oxygen consumption and the decay of the growth factor. The MDGF production rate Q depends on the oxygen concentration in the following way

$$Q(u_1) = \begin{cases} 0, & \text{if } x \in \Omega_u \\ 0, & \text{if } u_1 \geq u_\theta \\ 1 - \frac{u_1}{u_\theta}, & \text{if } u_1 < u_\theta, \end{cases}$$

where u_θ is some threshold value for the MDGF production and $\Omega_u = \Omega \setminus \Omega_w$, the unwounded skin surrounding the wound area. So the production of MDGF drops linearly to zero when the oxygen concentration is below the threshold value u_θ and rising.

The last term in (2.12) stands for the formation of new capillaries, where u_3^{eq} is the equilibrium cappilary density. New capillaries are more easily formed if there are already capillaries present, furthermore the presence of MDFGs also triggers the production. The term $\lambda_{13} u_3$ in (2.10) captures the transport of oxygen towards the wound, which is larger if there are more capillaries.

Initially the oxygen concentration is zero inside the wound are, i.e. Ω_w, and at its equilibrium in the rest of the computational domain, $\Omega_u = \Omega \setminus \Omega_w$. The same is assumed for the capillary density and also both u_1 and u_3 satisfy no-flux boundary conditions. The MDGF concentration, u_2, is assumed to be zero throughout the entire computational domain at time $t = 0$, furthermore it also satisfies a no-flux boundary condition.

2.2.2 Gaffney et al

The model proposed in [5] by Gaffney et al. takes a completely different strategy to model angiogenesis. It models the relation between the tip concentration and the endothelial cell density, which is a building block for new blood capillaries, [8]. I does not take into account the relation between shortage of oxygen and growth of new capillaries.

The model tries to capture the process where endothelial cells migrate out of blood vessels facing the wound. As they migrate they form a tube that extends

from the parent vessel, [8]. At the tips of these tubes cells proliferate to form new capillaries that extend into the wound area. Tips branch and join and thus form a new network of capillaries, from which the process is repeated.

If we let $n(x,t)$ and $b(x,t)$ be the tip concentration and the endothelial cell density respectively, then the partial differential equations of this model read

$$\frac{\partial n}{\partial t} = \nabla \cdot \{D_1 \nabla n + D_2 n \nabla b\} + f(n,b) \tag{2.13}$$

$$\frac{\partial b}{\partial t} = \lambda_1 \nabla \cdot \{D_1 \nabla n + D_2 n \nabla b\} + g(n,b). \tag{2.14}$$

The first term on the right hand side in both equations denotes transport as well as an additional migration towards a decreasing blood vessel density, [8]. The two functions f and g both depend on the tip concentration and the endothelial cell density. They represent production and decay of $n(x,t)$ and $b(x,t)$ respectively.

For the tip concentration $n(x,t)$ growth is due to tip branching, the splitting of tips into new tips. Decay can either be a result of two tips meeting at one point or a tip meeting a capillary. Since the probability that a tip is located at a certain point is proportional to n, the growth term is also proportional to n. Decay due to two tips meeting then is proportional to n^2, whereas decay from a tip meeting a capillary is proportional to nb. All this combined results in f being of the form

$$f(n,b) = \lambda_2 n - \lambda_3 n^2 - \lambda_4 nb. \tag{2.15}$$

The function $g(n,b)$ can be split into four seperate terms. The first denoting proliferation due to logistic growth of the endothelial cell density, [8]. The second term accounts for extra growth due to the presence of tips, which are build from endothelial cells. The third and fourth term are taken together and represent growth due to two tips joining or one tip merging with a capillary (compare to the last two terms in (2.15)). The whole function g is thus given by

$$g(n,b) = \lambda_6 ab(b_0 - b) + \lambda_6 \chi nb(b_1 - b) + \lambda_5(\lambda_3 n^2 + \lambda_4 nb). \tag{2.16}$$

At the boundary of the computational domain Ω it is assumed that no transport takes place of both tips and endothelial cells, so they both satisfy a no-flux boundary condition. Furthermore it is assumed that inside the wound area, $x \in \Omega_w$, there are no tips and endothelial cells present initially. Outside the wound area, the endothelial cell concentration is at its equilibrium due to the undamaged capillaries. The tip concentration is everywhere zero, except for a small strip facing the wound area.

2.3 Wound closure

The final stage of the healing process is closure of the wound. When the wounded area has been sufficiently supplied with oxygen and nutriciens, cells in the epidermis start dividing and so regenerate the lost skin as good as possible. This process is triggered by numerous growth factors, but in the following two models

it is assumed that only one generic growth factor influences wound closure, [8]. Note that this process takes place in the epidermis, unlike wound contraction and angiogenesis.

2.3.1 Sherratt and Murray

If the density of epidermal cells is low, the production of the epidermal cell derived growth factor is high. And under the influence of the growth factor the production of epidermal cells increases. Those are the basics for the model due to Sherratt and Murray proposed in [6]. As the wound heals, the production of epidermal cells descreases to a point where the proliferation rate is in balance with the decay rate, [8].

If we let u_4 denote the epidermal cell density then its balance is given by

$$\frac{\partial u_4}{\partial t} = D_4 \Delta u_4 + s(u_5) u_4 \left[2 - \frac{u_4}{u_4^{\text{eq}}} \right] - \lambda_{44} u_4, \tag{2.17}$$

where the terms on the right hand side account for diffusive transport, proliferation and cell death respectively. The growth factor concentration is denoted by u_5 and s is a nonlinear function of this concentration describing the mitotic rate.

Sherratt and Murray consider two different types of growth factors, activators and inhibitors. The function $s(u_5)$ is different in both cases and reads

$$s(u_5) = \frac{2c_m(h-\beta)u_5}{c_m^2 + u_5^2} + \beta \tag{2.18}$$

for the activator and

$$s(u_5) = \frac{(h-1)u_5 + h}{2(h-1)u_5 + 1} \tag{2.19}$$

for the inhibitor, here h and c_m are known constants and

$$\beta = \frac{1 + c_m^2 - 2hc_m}{(1-c_m)^2}$$

The function $s(u_5)$ is plotted in Figure 2.1 for $h = 10$ and $c_m = 40$.

The growth factor concentration behaves similarly to (2.17) and thus for u_5 we obtain

$$\frac{\partial u_5}{\partial t} = D_5 \Delta u_5 + f(u_4) - \lambda_{55} u_5. \tag{2.20}$$

Here the function f is a nonlinear function of u_4, which is also different in the activator and inhibitor case. For the activator case it is given by

$$f(u_4) = \frac{u_4(1+\alpha^2)}{u_4^2 + \alpha^2}, \tag{2.21}$$

where α is a constant, and for the inhibitor it is given by

$$f(u_4) = u_4. \tag{2.22}$$

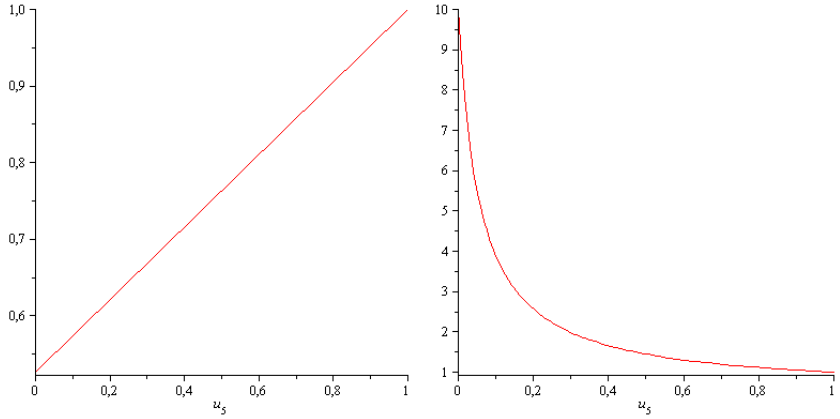

Figure 2.1: The function $s(u_5)$ for an activator (left) and an inhibitor (right).

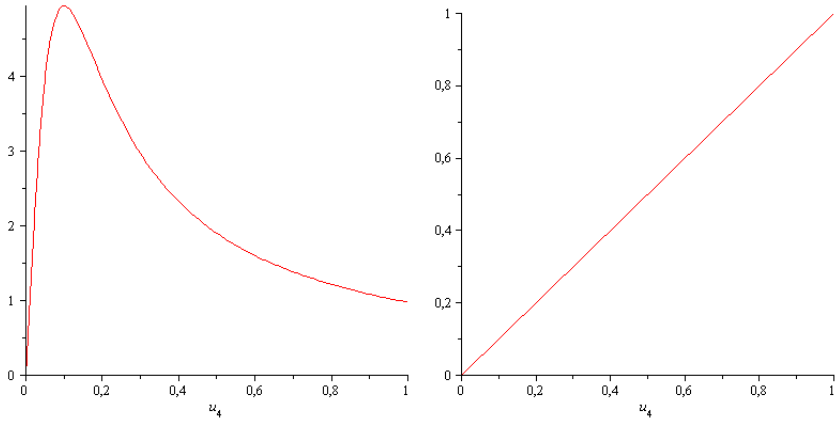

Figure 2.2: The function $f(u_4)$ for an activator (left) and an inhibitor (right).

The function $f(u_4)$ is plotted in Figure 2.2 for $\alpha = 0.1$.

For both the epidermal cell density and the growth factor concentration the initial value is zero inside the wound and both are at their equilibrium outside the wound are, i.e.

$$u_4(\mathbf{x}, 0) = \begin{cases} 0, & \text{for } \mathbf{x} \in \Omega_w \\ u_4^{\text{eq}}, & \text{for } \mathbf{x} \in \Omega_u \end{cases}$$
$$u_5(\mathbf{x}, 0) = \begin{cases} 0, & \text{for } \mathbf{x} \in \Omega_w \\ u_5^{\text{eq}}, & \text{for } \mathbf{x} \in \Omega_u. \end{cases}$$

Furthermore it is assumed that there is no transport of both epidermal cells and growth factor over the boundaries of the computational domain. Thus a no-flux boundary condition is induced on both u_4 and u_5.

2.3.2 Adam

The model due to Adam, proposed in [7], takes a somewhat different approach as it only considers the dynamics of the growth factor concentration. Then based on the presence of the growth factor the healing process is described, [8].

Firstly, the computational domain Ω is split up in three subdomains $\Omega_1(t)$, $\Omega_2(t)$ and $\Omega_3(t)$. They denote the wound area, the active layer and the outer (healthy) tissue respectively and are functions of time since the wound is healing.

The presence of growth factor is influenced by diffusive transport, decay and production. If we denote its concentration by c, the partial differential equation for the growth factor is given by

$$\frac{\partial c}{\partial t} = \nabla \cdot (D \nabla c) - \lambda c + P \mathbf{1}_{\Omega_2}, \tag{2.23}$$

where D, λ and P are the diffusion coefficient, decay factor and production rate respectively. Furthermore

$$\mathbf{1}_{\Omega_2} = \begin{cases} 1, & \text{for } \mathbf{x} \in \Omega_2(t) \\ 0, & \text{for } \mathbf{x} \in \Omega_1(t) \cup \Omega_3(t), \end{cases} \tag{2.24}$$

the indicator function of $\Omega_2(t)$. On the boundary $\partial\Omega$ we assume no transport of the growth factor and thus a no-flux boundary condition is imposed. Initially the growth factor is assumed to be absent in the entire computational domain, [8].

If we denote the interface between $\Omega_1(t)$ and $\Omega_2(t)$ by $W(t)$,

$$W(t) = \bar{\Omega_1}(t) \cup \bar{\Omega_2}(t), \tag{2.25}$$

then healing at a certain location on $W(t)$ implies that the inward normal component of the velocity, v_ν, is positive, [8]. The model due to Adam, see [7], says that this is so when the growth factor concentration exceeds a certain value, i.e. $v_\nu \neq 0$ if and only if $c(x,t) > \hat{c}$, for x on the interface $W(t)$.

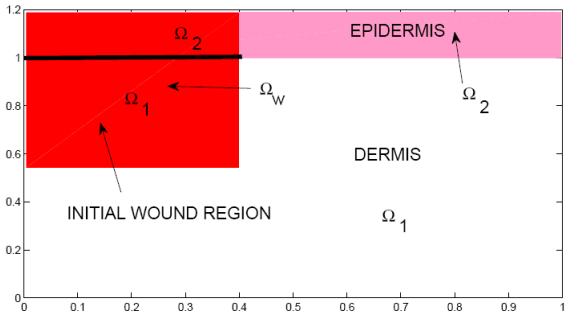

Figure 2.3: The geometry of the model with the dermis and the epidermis. This figure was taken, with permission, from [9].

Furthermore it is assumed that the healing rate is proportional to the local curvature κ of the wound. Then the velocity component in the outward (from $\Omega_1(t)$) normal direction is given by

$$v_\nu = -(\alpha + \beta\kappa)w(c(t, \mathbf{x}) - \hat{c}). \tag{2.26}$$

Here α and β are positive constants, prohibiting growth of the wound if $\kappa \geq 0$, and $w(s)$ falls within the family of Heaviside functions.

So to know if the wound is healing at a certain location along the interface $W(t)$, one needs to know the growth factor concentration there. To know the rate of healing, one must look at the curvature of the wound.

2.4 Vermolen and Javierre

The models described in the previous sections all account for a single stage in the wound healing process. In fact these stages (partially) overlap each other in the healing process and thus are also influenced by one another. Furthermore where wound contraction occurs in the whole wound, angiogenesis and wound closure are dermal and epidermal processes respectively.

In [9] an attempt is made to combine models of the three stages to get more insight in the wound healing process, such as geometry influences. The model due to Murray and Tranquillo, see section 2.1.1, is used for wound contraction. For angiogenesis and wound closure the model due to Maggelakis, see section 2.2.1, and Sherratt and Murray, see section 2.3.1, are used respectively. Furthermore they consider a computational region in which there is a clear difference between the dermis and the epidermis, so that angiogenesis and wound closure can be simulated in seperate regions. In Figure 2.3 the computational region is depicted.

The results in [9] show a clear sequence of the above mentioned stages of wound healing. Also, they partially overlap (although the amount of overlapping does depend on the choice of parameters) and thus might influence one another, see Figures 2.4 and 2.5. These influences are not yet taken into account in this

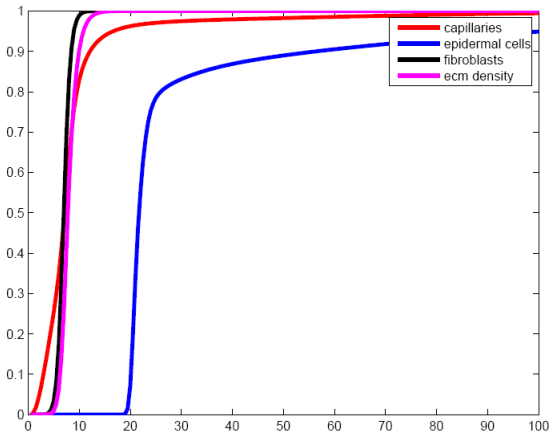

Figure 2.4: The concentration in the upper left part of the wound: capillary, ECM and fibroblast densities in the dermis, epidermal cell density in the epidermis. Here the capillary diffusity was taken $D_c = 0.01$ cm^2/s. This figure was taken, with permission, from [9].

model and are topics for future research. For more details and results we refer to [9].

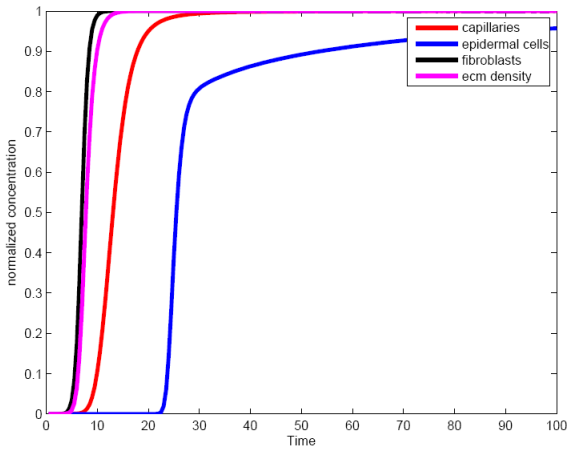

Figure 2.5: The concentration in the upper left part of the wound: capillary, ECM and fibroblast densities in the dermis, epidermal cell density in the epidermis. Here the capillary diffusity was taken $D_c = 0.001$ cm^2/s. This figure was taken, with permission, from [9].

Chapter 3

Simulations of wound healing

In this section we present some computational results done on the models described in Chapter 2. For each stage in wound healing simulations have been done with one model. First the model due to Murray and Tranquillo is considered, second the model due to Maggelakis and finally the model due to Sherrat and Murray. This was done to give some understanding on how each stage in the wound healing process evolves.

The solutions have been obtained using the numerical methods described in Section 3.1 and the programming has been done in Matlab ©.

3.1 Numerical methods

In this section we show, using one equation as an example, how the computations on the models have been done. We consider the nonlinear reaction-diffusion equation

$$\frac{\partial u}{\partial t} = D\Delta u + \lambda u(1-u) \qquad \text{for } (\mathbf{x},t) \in \Omega \times [0,T], \tag{3.1}$$

subject to

$$\begin{aligned} \frac{\partial u}{\partial n} &= 0 \qquad \text{for } (\mathbf{x},t) \in \partial\Omega \times [0,T], \\ u(0,\mathbf{x}) &= u_0(\mathbf{x}). \end{aligned}$$

Here D and λ are constants and n denotes the outward normal vector. Furthermore note that u is in no way related to any of the variables used in the models described in Chapter 2.

To discritize the equation we are going to use the Finite Element Method (FEM). We multiply (3.1) by a testfunction η and integrate over the computa-

tional domain Ω to obtain

$$\int_\Omega \frac{\partial u}{\partial t}\eta\partial\Omega = \int_\Omega D\eta\Delta u + \lambda u(1-u)\eta\partial\Omega. \tag{3.2}$$

To the first term on the right hand side we apply the product rule for differentation and Gauss' Theorem, which gives us

$$\int_\Omega \frac{\partial u}{\partial t}\eta\partial\Omega = \int_\Omega -D\nabla\eta\cdot\nabla u + \lambda u(1-u)\eta\partial\Omega + D\int_{\partial\Omega}\eta\nabla u\cdot\mathbf{n}\partial\Gamma, \tag{3.3}$$

where the last term on the right hand side is equal to zero due to the boundary condition.

Now we use Galerkin's method and approximate u by

$$u^N = \sum_{j=1}^{N} u_j(t)\phi_j(\mathbf{x}). \tag{3.4}$$

The function $\phi_j(\mathbf{x})$ must be sufficiently smooth and must satisfy the same boundary conditions as u. Furthermore we also want the testfunction η to be a linear combination of $\phi_j(\mathbf{x})$, i.e.

$$\eta = \sum_{j=1}^{N} b_j\phi_j(\mathbf{x}). \tag{3.5}$$

This is natural since the testfunction is in the same space as u. As η is chosen arbitrarily, we can assume that all b_j are equal to zero except for one $b_i = 1$. Using this and substituting (3.4) and (3.5) into (3.2) results in

$$\frac{d}{dt}\sum_{j=1}^{N} u_j\int_\Omega \phi_j\phi_i\partial\Omega = -D\sum_{j=1}^{N} u_j\int_\Omega \nabla\phi_j\cdot\nabla\phi_i\partial\Omega + \lambda\sum_{j=1}^{N} u_j\int_\Omega (1-u)\phi_j\phi_i\partial\Omega \tag{3.6}$$

for $i = 1\ldots N$. The term $1-u$ in the right hand side will be evaluated at the previous timestep.

Note that (3.6) can be written in matrix-vector form

$$M\frac{d\bar{u}}{dt} = S(u)\bar{u} + f, \tag{3.7}$$

where $\bar{u} = [u_1, u_2, \ldots, u_N]^T$. We will omit the bar from now on and just write u. The matrix M (time matrix) contains the integrals in the left hand side of (3.6),

$$M_{ij} = \int_\Omega \phi_i\phi_j\partial\Omega,$$

whereas $S(u)$ (mass matrix) contains the integrals on the right hand size

$$S(u)_{ij} = -D\int_\Omega \nabla\phi_j\cdot\nabla\phi_i\partial\Omega + \lambda\int_\Omega (1-u)\phi_i\phi_j\partial\Omega.$$

In this case $f = \mathbf{0}$. Now we split the domain Ω up into (triangular) elements e_k and can construct the time and mass matrix using element matrices, see [10] for more details.

Let us denote the element time and mass matrix by M_e and S_e respectively. For the $\phi_j(\mathbf{x})$ we have used the linear basisfunctions. The elements of M_e are then given (for $i, j = 1 \dots 3$), using Newton-Cotes for a triangle with linear basisfunctions, by

$$\begin{aligned} M_e^{ij} &= \int_e \phi_i \phi_j de \\ &= \sum_{k=1}^{3} \phi_i(\mathbf{x}_k)\phi_j(\mathbf{x}_k) \int_e \phi_k de \\ &= \delta_{ij} \frac{|\Delta|}{6}, \end{aligned}$$

where we have used local numbering ($\mathbf{x}_1$, $\mathbf{x}_2$ and $\mathbf{x}_3$ denote the corners of the triangle) and Δ denotes the surface of the element. The elements of S_e are given by

$$S(u)_e^{ij} = -D \int_e \nabla\phi_i \cdot \nabla\phi_j de + \lambda \int_e (1-u)\phi_i\phi_j de, \tag{3.8}$$

for $i, j = 1 \dots 3$. In a similar way as done with the elements of M_e we can use Newton-Cotes to approximate the elements of S_e and find

$$S(u)_e^{ij} = -D\frac{|\Delta|}{2}(a_1^i a_1^j + a_2^i a_2^j) + \lambda(1 - u(\mathbf{x}_i))\frac{|\Delta|}{6}\delta_{ij}, \tag{3.9}$$

where a_l^k ($k = 1 \dots 3$, $l = 1, 2$) are derivatives of the linear basisfunctions and can be found in [10] at page 105.

We have now constructed the matrices M and $S(u)$ from the matrix-vector equation (3.7). In this case the vector $f = \mathbf{0}$ and we are left with

$$M\frac{du}{dt} = S(u)u. \tag{3.10}$$

To solve u from this matrix-vector equation we now must integrate in time. We will denote u^m as the solution at time $t = t_m = m\Delta t$, where Δt is the timestep. Using Crank-Nicolson for the time integration yields

$$\left(M - \frac{1}{2}\Delta t S(u^m)\right) u^{m+1} = \left(M + \frac{1}{2}\Delta t S(u^m)\right) u^m. \tag{3.11}$$

Note that S is a function of the solution at the previous timestep, this is due to the nonlinear term $1 - u$ in (3.1). This leaves us with a matrix-vector equation for each timestep. This type of equation is easily solved in Matlab, especially as M and S are sparse matrices.

production rates	$b,\ r$	$1,\ 1$
equilibrium values	$\rho_0,\ n_0$	$1,\ 1$
diffusive coefficient	D_n	0.1
Young's modulus	E	10^6
Poisson ratio	ν	0.25
shear and bulk viscosity	$\mu_1,\ \mu_2$	$10^6,\ 10^6$
thetering elasticity coefficient	s	10^6
other constants	$\tau,\ \lambda$	$0.5,\ 1$
timestep	Δt	0.01

Table 3.1: Parameters used in simulation of the model due to Murray and Tranquillo.

3.2 Model due to Murray and Tranquillo

In this section we discuss the results of the simulation of the model due to Murray and Tranquillo. We consider the computational domain (dermis) $\Omega = [0,1] \times [0,1]$ and a wound region $\Omega_w = \{\mathbf{x} :\ |\mathbf{x}| < 0.5\}$. Further parameters values can be found in Table 3.1. Initially both fibroblasts and the extra cellular matrix (ECM) are absent inside the wound. As time progresses fibroblasts invade the wound, see Figure 3.1. Due to diffusive transport the fibroblast concentration decreases in the surrounding (healthy) tissue, whereas the concentration increases inside the wound.

Shortly after the fibroblast have entered the wound ECM starts forming. As the ECM is non-motile (it only moves due to passive movement) the density outside the wound remains at its equilibrium. Inside the wound the ECM density starts increasing in a similar way as the fibroblast concentration, see Figure 3.2.

The computation shows what one would expect to happen. After the injury has occured, the wound is void of both fibroblast and ECM. The fibroblast then move in to restore the ECM, so that angiogenesis can take place.

3.3 Model due to Maggelakis

For the angiogenesis stage of the healing process we have chosen to use the model due to Maggelakis. This model, unlike the model due to Gaffney et al, incorporates the effects of lack of oxygen on the growth of new capillaries. This is considered as an important aspect of angiogenesis.

We consider the same computational domain (dermis) and wound area as in Section 3.2. The parameters values used in the simulation can be found in Table 3.2.

Figure 3.3 shows the MDGF (macrophage derived growth factor) concentration at three different (successive) timesteps. Initially this concentration is zero everywhere in the computational domain. Due to the lack of oxygen it starts increasing, but only in the wound area (in the undamaged tissue there is no lack

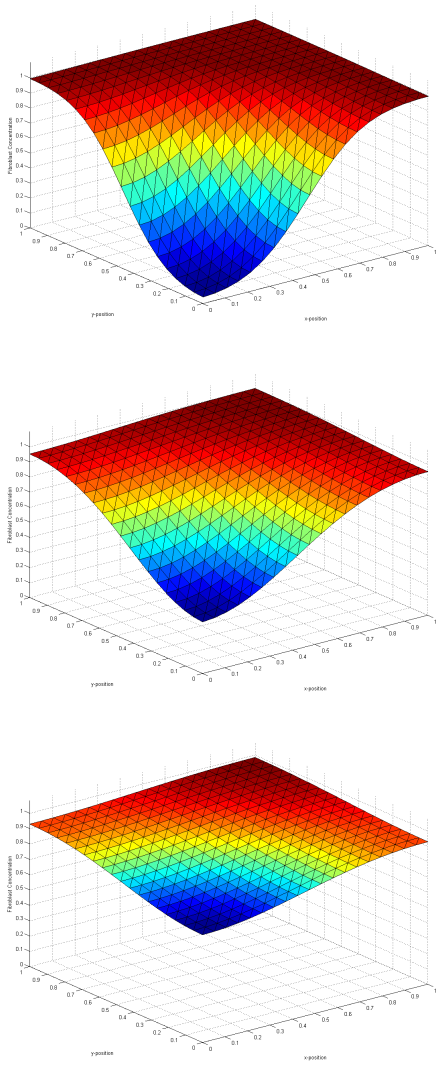

Figure 3.1: Fibroblast concentration after respectively 20 (top), 50 (middle) and 100 (bottom) time steps.

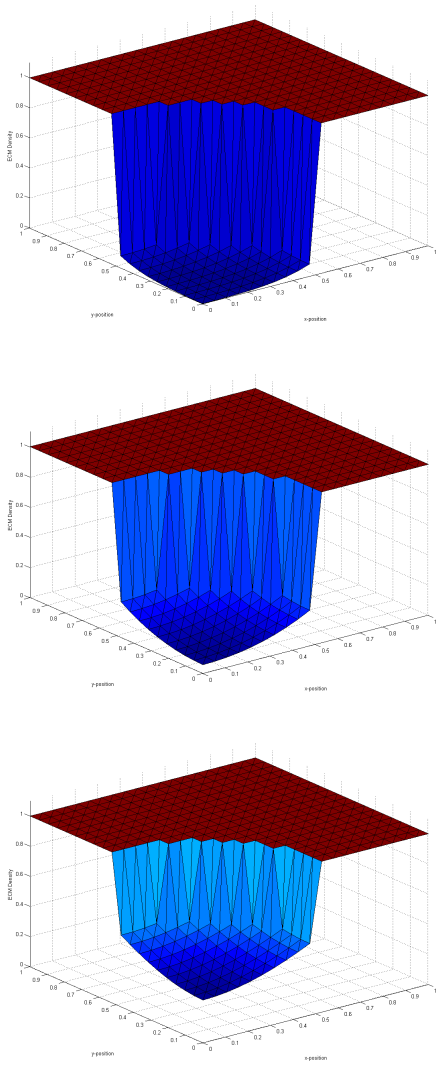

Figure 3.2: ECM density after respectively 20 (top), 50 (middle) and 100 (bottom) time steps.

diffusive coefficients	$D_1,\ D_2,\ D_3$	$0.01,\ 0.1,\ 0.01$
decay factors	$\lambda_{11},\ \lambda_{22}$	$0.02,\ 1$
oxygen transport rate	λ_{13}	1
MDGF production rate	λ_{21}	10
capillary production rate	λ_{33}	10
capillary density equilibrium	u_3^{eq}	0.1
oxygen concentration equilibrium	u_θ	5
timestep	Δt	0.01

Table 3.2: Parameters used in simulation of the model due to Maggelakis.

diffusive coefficients	$D_4,\ D_5$	$5 \cdot 10^{-4},\ 0.45$
decay factors	$\lambda_{44},\ \lambda_{55}$	$1,\ 1$
epidermal cell density equilibrium	u_4^{eq}	1
growth factor concentration equilibrium	u_5^{eq}	1
other constants	$c_m,\ h,\ \alpha$	$40,\ 10,\ 0.1$
timestep	Δt	0.01

Table 3.3: Parameters used in simulation of the model due to Sherratt and Murray.

of oxygen). As a result of diffusive transport the MDGF spreads over the entire domain, but remains at its peak in the wound area.

The capillary density inside the wound is zero at $t = 0$ (there are no blood vessels remaining after injury). When the MDGF concentration rises it triggers the production of new capillaries and so the capillary density increases. Already after 50 timesteps the capillary density is almost at its equilibrium, as can be seen in Figure 3.4. When it has reached a stable state (after 80 timesteps) the growth of new capillaries is stopped and the density remains at its equilibrium.

When new capillaries are formed oxygen can once again be transported to the wounded area. Initially the concentration is zero inside the wound, but as more capillaries are formed the concentration increases. Although this process happens rather slowly, it can be seen in Figure 3.5 that the oxygen concentration does rise towards an equilibrium.

3.4 Model due to Sherratt and Murray

In this section we consider the wound closure model due to Sherratt and Murray. This model describes the relation between the growth factor concentration and the epidermal cell density. We chose to compute the model with an activator as growth factor, then the growth factor triggers the profileration of epidermal cells.

We consider the computational domain (epidermis) $\Omega = [0, 1] \times [0, 1]$ and a wound region $\Omega_w = \{\mathbf{x} :\ |\mathbf{x}| < 0.5\}$. Further parameter values that were used in the computation can be found in Table 3.3.

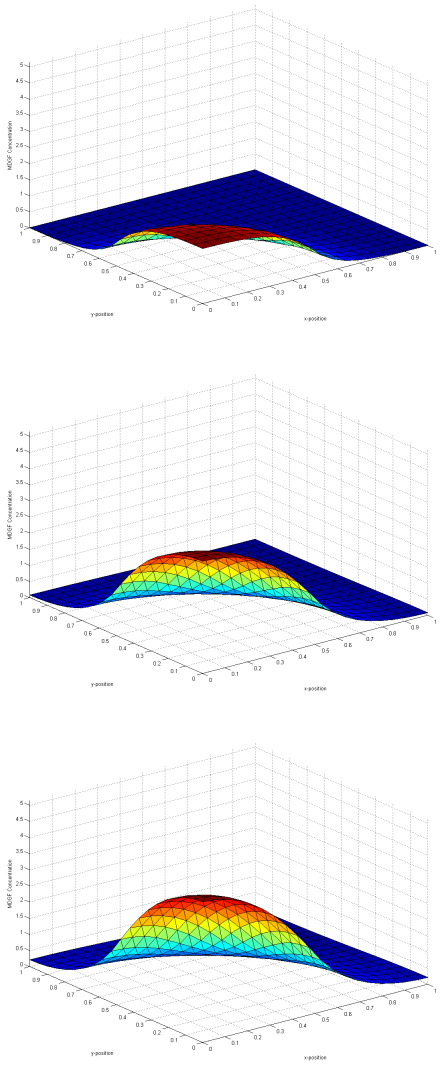

Figure 3.3: MDGF concentration after respectively 20 (top), 50 (middle) and 80 (bottom) time steps.

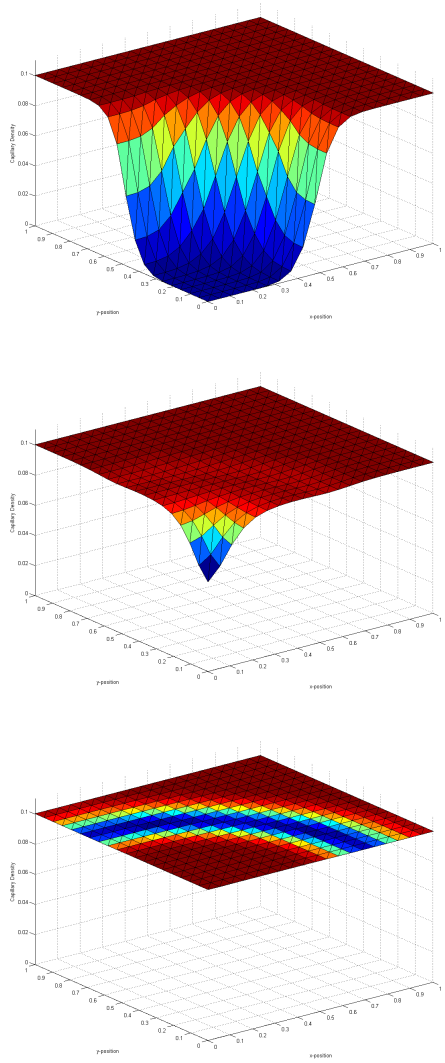

Figure 3.4: Capillary density after respectively 20 (top), 50 (middle) and 80 (bottom) time steps.

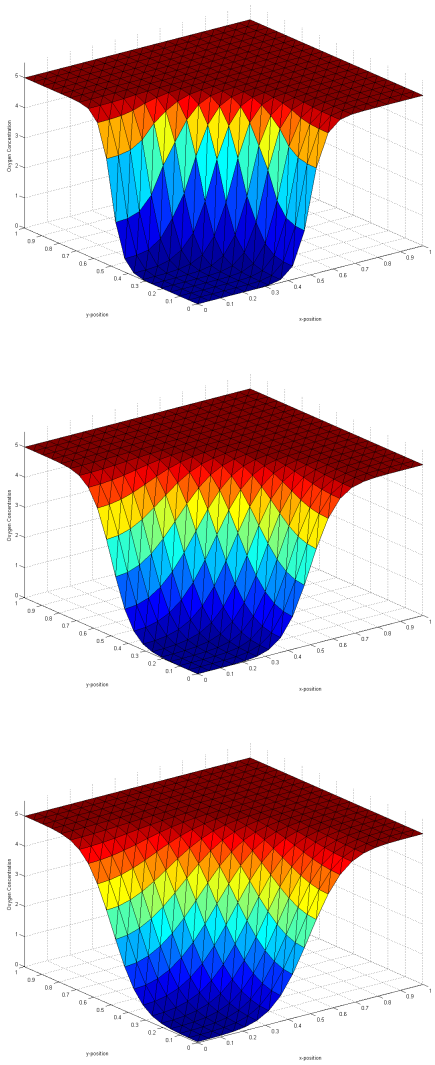

Figure 3.5: Oxygen concentration after respectively 20 (top), 50 (middle) and 80 (bottom) time steps.

The growth factor concentration is assumed to initially be at its equilibrium outside the wound and zero inside the wound. The concentration drops somewhat at first, but starts rising again to even above the equilibrium. The concentration has an elevation at the wound edge where the skin starts recorvering first, see Figure 3.6.

The epidermal cell density also drops somewhat at first, see Figure 3.7. But after some time it starts rising througout the domain, but mostly at the wound edge. Since the growth factor concentration is elevated at here, the most proliferation takes place at the wound edge. So just as one would expect, the wound closes from the edge towards the center.

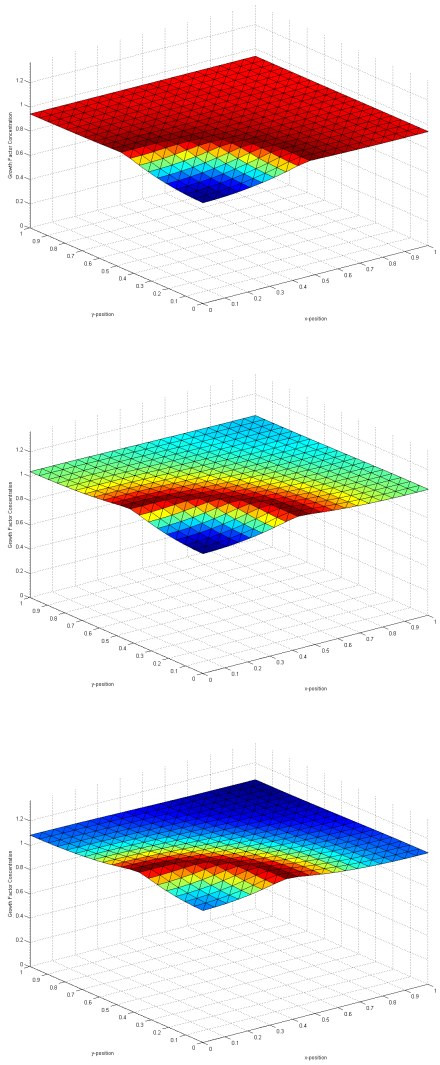

Figure 3.6: Growth factor concentration after respectively 100 (top), 200 (middle) and 300 (bottom) time steps.

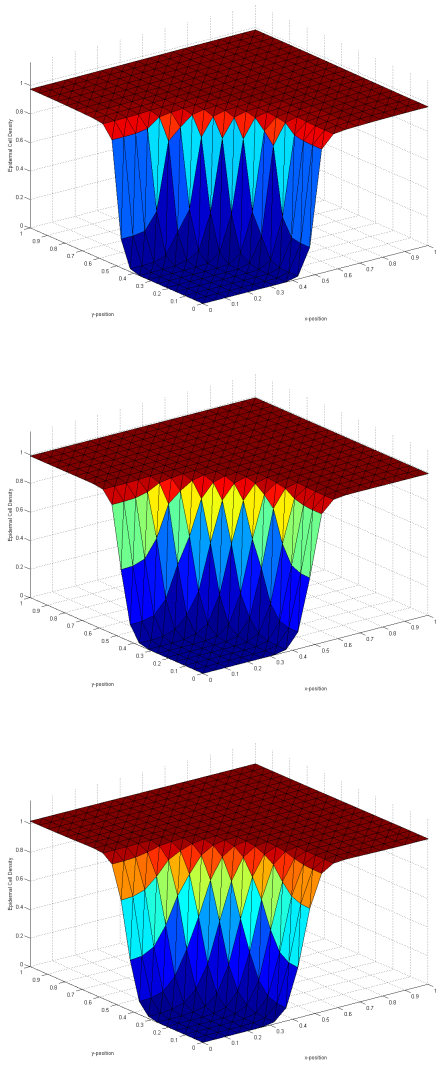

Figure 3.7: Epidermal cell density after respectively 100 (top), 200 (middle) and 300 (bottom) time steps.

Chapter 4

Conclusions and future work

The wound healing process can be divided in three stages, i.e. wound contraction, angiogenesis and wound closure. For each separate stage there are currently several different models available. These are to some extent reasonable depictions of the real process.

In reality, of course, these seperate stages overlap, as is already shown in [9]. Furthermore they influence each other, e.g. epidermal cells proliferate much more slowly with a lack of oxygen. Also angiogenesis might have significant influences on wound contraction. Such coupling between the models of seperate stages are topics for future study.

Another issue concerns the two different models for angiogenesis. The model due to Maggelakis approaches angiogenesis as a process where oxygen shortage results in growth of new capillaries via a (growth factor based) trigger mechanism. The model due to Gaffney et al ignores the effects of oxygen shortage on capillary growth. But it does capture quite well the process on how new capillaries are formed out of other, already present, blood vessels.

It might be interesting to combine these two models, so that both aspects of capillary growth are incorporated. This could give a better insight on how the process of angiogenesis works.

As said, a lot of work can still be done on the topic of wound healing. For future research we would recommend

1. Combination of the models for angiogenesis due to Maggelakis and Gaffney et al.

2. Combination of the new model for angiogenesis with the model for wound conctraction.

3. Combination of the angiogenesis and wound contraction model with wound closure.

4. Modelling of the position of the basal membrane, which separtes the dermis from the epidermis.

Bibliography

[1] V. Kumar, A. Abbas and N. Fausto: *Robbins and Cotran Pathologic Basis of Disease*, ISBN 0-7216-0187-1

[2] J.D. Murray: *Mathematical Biology II: Spatial Models and Biomedical Applications*, ISBN 0-387-95228-4

[3] L. Olsen, J.A. Sherratt and P.K. Maini: *A mechanochemical model for adult dermal wound closure and the permanence of contracted tissue displacement*

[4] S.A. Maggelakis: *A mathematical model for tissue replacement during epidermal wound healing*

[5] E.A. Gaffney, K. Pugh and P.K. Maini: *Investigating a simple model for cutaneous wound healing angiogenesis*

[6] J.A. Sherrat and J.D. Murray: *Mathematical analysis of a basic model for epidermal wound healing*

[7] J.A. Adam: *A simplified model of wound healing (with particular reference to the critical size deffect)*

[8] F.J. Vermolen and E. Javierre: *A suite of continuum models for different aspects in wound healing*

[9] F.J. Vermolen and E. Javierre: *Computer simulations from a finite-element model for wound contraction and closure*

[10] J. van Kan, A. Segal and F.J. Vermolen: *Numerical Methods in Scientific Computing*, ISBN 90-71301-50-8